

Orchestration of the Floral Transition and Floral Development in *Arabidopsis* by the Bifunctional Transcription Factor APETALA2

Levi Yant,^{a,1} Johannes Mathieu,^{a,2} Thanh Theresa Dinh,^{b,c} Felix Ott,^a Christa Lanz,^a Heike Wollmann,^{a,3} Xuemei Chen,^b and Markus Schmid^{a,4}

^aMax Planck Institute for Developmental Biology, D-72076 Tübingen, Germany

^bDepartment of Botany and Plant Sciences, Center for Plant Cell Biology, Institute of Integrative Genome Biology, University of California, Riverside, California 92521

^cChemGen IGERT Program, Center for Plant Cell Biology, Institute of Integrative Genome Biology, University of California, Riverside, California 92521

The *Arabidopsis thaliana* transcription factor APETALA2 (AP2) has numerous functions, including roles in seed development, stem cell maintenance, and specification of floral organ identity. To understand the relationship between these different roles, we mapped direct targets of AP2 on a genome-wide scale in two tissue types. We find that AP2 binds to thousands of loci in the developing flower, many of which exhibit AP2-dependent transcription. Opposing, logical effects are evident in AP2 binding to two microRNA genes that influence AP2 expression, with AP2 positively regulating miR156 and negatively regulating miR172, forming a complex direct feedback loop, which also included all but one of the AP2-like miR172 target clade members. We compare the genome-wide direct target repertoire of AP2 with that of SCHLAFMÜTZE, a closely related transcription factor that also represses the transition to flowering. We detect clear similarities and important differences in the direct target repertoires that are also tissue specific. Finally, using an inducible expression system, we demonstrate that AP2 has dual molecular roles. It functions as both a transcriptional activator and repressor, directly inducing the expression of the floral repressor *AGAMOUS-LIKE15* and directly repressing the transcription of floral activators like *SUPPRESSOR OF OVEREXPRESSION OF CONSTANS1*.

INTRODUCTION

For both plants and animals, the timing of the transition from immature to reproductive growth must be tightly regulated to maintain its adaptive value. In flowering plants, for example, a diminished competence for tracking environmental cues and responding appropriately is correlated with declining species abundance or even extinction (Willis et al., 2008). It is therefore no surprise that a finely nuanced gene regulatory network evolved to translate environmental and endogenous information, integrate the diverse inputs, and commit resources to initiate flowering when the time is most favorable. The emerging view of the

regulatory network governing the reproductive transition in *Arabidopsis thaliana* is that of a tuned balance of repressors and activators, both classes operating throughout the plant tissues and at every level in the flowering time network topology (Kobayashi and Weigel, 2007; Giakountis and Coupland, 2008; Yant et al., 2009). Both positive and negative inputs are conveyed along initially distinct, but later crosstalking pathways to the shoot apex, where the transition is finally realized in morphological changes.

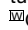
Extensive genetic and molecular studies have described several cardinal flowering time pathways: the photoperiod, vernalization, gibberellic acid, and autonomous pathways, each of which exerts either a floral promoting, neutral, or inhibiting state at any given time in response to different cues. The photoperiod pathway, for example, measures light quantity and quality in the leaves and promotes flowering as soon as daylength, or photoperiod, meets a particular threshold. When this threshold photoperiod is sensed, *FLOWERING LOCUS T (FT)* expression is upregulated in the leaves. The FT protein is then thought to travel to the shoot apex (Jaeger et al., 2006; Lifschitz et al., 2006; Corbesier et al., 2007; Jaeger and Wigge, 2007; Mathieu et al., 2007; Tamaki et al., 2007; Komiya et al., 2009), where it interacts with the bZip transcription factor FD to orchestrate the transition to flowering, including the expression of the MADS domain protein APETALA1 (AP1) (Abe et al., 2005; Wigge et al., 2005).

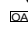
¹ Current address: Department of Organismic and Evolutionary Biology, Harvard University, Cambridge, MA 02138.

² Current address: Boyce Thompson Institute for Plant Research, Ithaca, NY 14853.

³ Current address: Chromatin and Reproduction Group, Temasek Life Sciences Laboratory, National University of Singapore, Singapore 117604, Singapore.

⁴ Address correspondence to markus.schmid@tuebingen.mpg.de. The authors responsible for distribution of materials integral to the findings presented in this article in accordance with the policy described in the Instructions for Authors (www.plantcell.org) are: Xuemei Chen (xuemei.chen@ucr.edu) and Markus Schmid (markus.schmid@tuebingen.mpg.de).

 Online version contains Web-only data.

 Open Access articles can be viewed online without a subscription www.plantcell.org/cgi/doi/10.1105/tpc.110.075606

Transcriptional repressors play a major role in flowering. The MADS domain transcription factor FLOWERING LOCUS C (FLC) represses *FT* expression and represents an important intersection of the photoperiod, vernalization, and autonomous pathways. FLC and another MADS domain transcription factor, SHORT VEGETATIVE PHASE, cooperate to repress directly the expression of the flowering pathway integrators *FT*, *FD*, and the MADS domain protein SUPPRESSOR OF OVEREXPRESSION OF CONSTANS1 (*SOC1*) by binding to their genomic loci (Lee et al., 2007; Li et al., 2008). Eventually this repressor, *FLC*, is itself repressed when plants experience extended periods of cold, or vernalization, during which an antisense RNA at the *FLC* locus (Swiezewski et al., 2009) initiates localized histone demethylase activity (Liu et al., 2010). In the absence of vernalization, inhibition of *FLC* expression is finally achieved later in development by members of the autonomous flowering pathway, *FCA* and *FY* (reviewed in Simpson et al., 2004), ensuring eventual flowering. In addition to this balancing act of *FT* promotion and transcriptional repression, another level of repression occurs when *FT* reaches the shoot apex. TERMINAL FLOWER1 (TFL1), itself a floral repressor with a high degree of homology to *FT* is thought to compete directly with *FT* for heterodimerization with *FD* at the shoot apex (Abe et al., 2005; Hanzawa et al., 2005; Wigge et al., 2005; Ahn et al., 2006; Giakountis and Coupland, 2008).

Aside from MADS domain repressors, another major group of transcriptional repressors plays a role in this complex network. It was recently discovered that the daylength-dependent upregulation of *FT* is directly repressed by AP2 domain-containing proteins from two related families. First, the TEMPRANILLO1 (TEM1) and TEM2 proteins were shown to repress flowering redundantly by repressing *FT* transcription (Castillejo and Pelaz, 2008). *TEM1* belongs to a family of RAV-like AP2-DNA domain-containing loci that encode proteins with an AP2 domain and a B3-type DNA binding domain. It is most strongly expressed in leaves, where it represses flowering by directly binding to the 5' untranslated region (UTR) of the *FT* genomic locus (Castillejo and Pelaz, 2008). A second, larger family of AP2-DNA domain-containing proteins is divided to two lineages: the *ANT* and euAP2 lineage (Kim et al., 2006). The euAP2 lineage contains six members that are predicted to be targeted by a major developmental microRNA and floral promoter, microRNA172 (miR172). This clade consists of the three TARGET OF EAT (TOE) genes (*TOE1* to *TOE3*), SCHLAFMÜTZE (*SMZ*), its paralog SCHNARCHZAPFEN (*SNZ*), and AP2 (Park et al., 2002; Aukerman and Sakai, 2003; Schmid et al., 2003).

Although pleiotropic functions have been obvious in the analysis of *ap2* mutants, the extensive redundancy among the AP2-like miR172 target clade members has long obscured their role in flowering time. Recent work has shown that overexpression of AP2, SMZ, SNZ, TOE1, or TOE2 caused late flowering (Aukerman and Sakai, 2003; Schmid et al., 2003; Chen, 2004; Jung et al., 2007) and that a quadruple *smz snz toe1 toe2* mutant flowered earlier than any single or double mutant (Jung et al., 2007; Mathieu et al., 2009). When expressed in the leaves, SMZ is capable of repressing flowering by directly binding to the *FT* genomic locus, although misexpression of SMZ at the shoot apex has a negligible effect on flowering time (Mathieu et al.,

2009). Therefore, given that AP2 is well known to be expressed and have functions in the shoot apex, we hypothesized that the partial redundancy observed among members of the clade may be due in part to tissue-specific expression of particular members, but also to differences in gene regulatory interactions with downstream targets.

AP2 is involved in a wide variety of developmental processes at the shoot apex, including the regulation of the stem cell niche (Wurschum et al., 2006), floral organ determination (Bowman et al., 1989), and the control of seed mass (Ohto et al., 2005). This extensive pleiotropy suggests a highly connected regulatory role (Carrera et al., 2009), the elucidation of which should be informative for understanding how AP2 influences such a variety of developmental processes.

Here, we describe repression of flowering by AP2 and its partially redundant family members, all targets of miR172. We reveal its mechanistic basis by high-resolution mapping of AP2 binding sites across the *Arabidopsis* genome and inducible gene expression analysis. AP2 represses flowering and flower development by binding directly to, and repressing the transcription of, the key flowering loci *SOC1* and *AGAMOUS* and by binding to the miR172 genomic locus and repressing its transcription. Surprisingly, AP2 also functions as a bifunctional transcription factor, directly activating other floral repressors, the MADS domain protein *AGAMOUS-LIKE15* (*AGL15*) (Adamczyk et al., 2007) and miR156 (Wang et al., 2009; Wu et al., 2009) by binding directly to their genomic loci.

RESULTS

AP2 Represses Flowering in a Daylength-Independent Manner

In addition to its better-known role in floral organ identity, a previous study indicated that AP2 was necessary for the late flowering induced by sucrose application (Ohto et al., 2001). When subjected to continuous light, an *ap2* mutant flowered earlier than did controls (Ohto et al., 2005). To investigate the effect of AP2 mutations on flowering time under more ecologically relevant daylengths, we obtained a strong AP2 T-DNA insertion allele (Alonso et al., 2003), SALK_071140 (hereafter called *ap2-12*). We found that the transition to flowering was accelerated in this *ap2* mutant under both noninductive short-day (SD; 8-h photoperiod) and inductive long-day (LD; 16-h photoperiod) conditions (Figure 1; see Supplemental Table 1 online). This effect was most marked under SD conditions, where the homozygous mutant produced only 25.3 ± 1.4 (2xSEM) leaves before flowering compared with wild-type Columbia-0 (Col-0) controls, which produced 47.8 ± 2.1 leaves ($P < 0.0001$, unpaired *t* test; Figure 1B). Under LD conditions, where the transition to flowering is greatly accelerated in *Arabidopsis*, *ap2-12* mutants still flowered early, producing 10.0 ± 0.5 leaves before flowering, compared with the wild type, which produced 13.5 ± 0.5 leaves ($P < 0.0001$, unpaired *t* test; Figure 1C). Direct sequencing of the *ap2-12* insertion site showed that the disruption was in the fifth intron, 18 nucleotides 5' from the exon boundary, and AP2 mRNA levels in the mutant were >16-fold lower than wild-type controls, as measured by quantitative

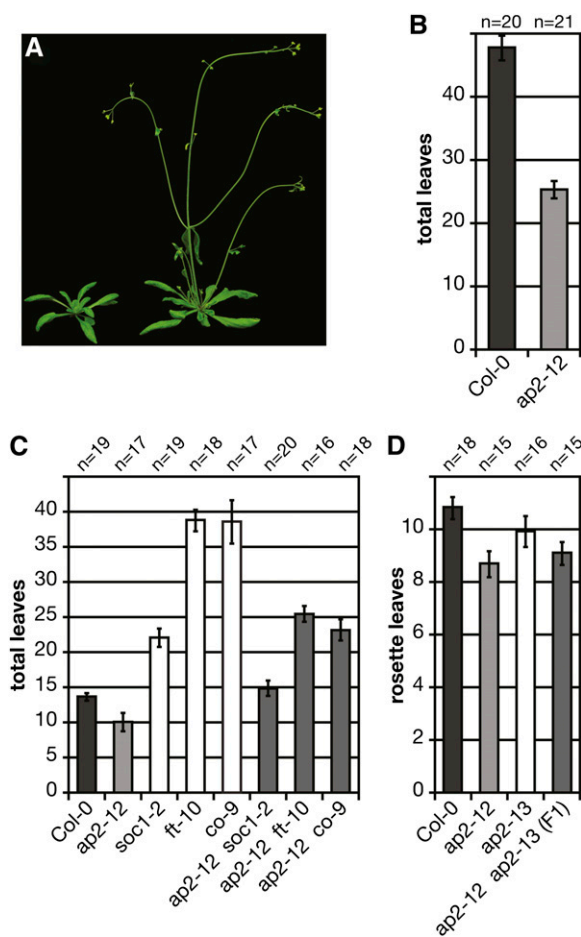


Figure 1. Influence of AP2 on Flowering Time and Genetic Interactions of AP2 with Other Flowering Time Mutants.

(A) Col-0 (left) and *ap2-12* (right) plants grown in LDs.

(B) *ap2-12* flowers early in SD conditions.

(C) *ap2-12* flowers early under LD conditions and attenuates all late flowering mutants tested.

(D) *ap2-12* and *ap2-13* exhibit a dosage-dependent effect and are allelic. F1 plants flower with an intermediate number of leaves.

In (A), (C), and (D), plants were grown in LD conditions. Flowering time is given as total leaf number (rosette leaves plus cauline leaves) in (B) and (C) and rosette leaf number in (D). Error bars indicate 2xSEM.

RT-PCR (qRT-PCR) (see Supplemental Figure 1 online). Flowers from *ap2-12* plants clearly exhibited the characteristic *ap2* loss-of-function phenotype.

To confirm further that the cause of early flowering was directly attributable to a lesion in *AP2* and not a second site mutation, we examined the flowering time of an independently derived *ap2* mutant allele. This line, *ap2-13*, was also early flowering, producing 11.8 ± 0.6 total leaves compared with the wild type (13.2 ± 0.4 ; total leaves in Supplemental Table 1 online, $P = 0.0013$, unpaired t test; rosette leaves in Figure 1D). F1 progeny of a cross of *ap2-12* and *ap2-13* all flowered early with an intermediate number of total leaves between the two parents (11.0 ± 0.4 ; see Supplemental Table 1 online). Thus, indepen-

dent lesions in *AP2* caused an early flowering phenotype, strongly implicating the loss of *AP2* itself as the cause of the early flowering. Furthermore, the intermediate flowering of the F1 progeny suggests a quantitative effect.

Because the closely related euAP2 clade member SMZ interacts with the photoperiod pathway to repress *FT* transcription directly (Mathieu et al., 2009), we investigated whether there might also be an interaction of *ap2* mutations with the photoperiod pathway. We therefore crossed *ap2-12* with late flowering mutants *soc1-2*, *ft-10*, and *co-9*, hypothesizing that the effect of losing a repressor will be more evident if the floral promoting stimulus is attenuated, similar to what we had observed in SD conditions. In all three late flowering backgrounds the effect of *ap2* loss of function was clear (Figure 1C; see Supplemental Table 1 online). In fact, *soc1-2 ap2-12* flowered only one leaf later than wild-type Col-0 plants, whereas *soc1-2* flowered 8.3 leaves later. When crossed to *ap2-12*, the strong mutants *ft-10* and *co-9* flowered 13.2 and 15.3 leaves earlier than the single mutant, respectively. Thus, the relative effect of *soc1*, *ft*, and *co* mutations was similar in the *ap2* mutant background, but the introduction of the *ap2* mutation produced additive early flowering in each line commensurate with the extent of late flowering in each single mutant. We conclude from these results that *AP2* acts as a bona fide floral repressor that delays flowering in *Arabidopsis* under both inductive and noninductive photoperiods.

Extreme Early Transition of the Hexuple AP2-Like miR172 Target Mutant

Including *AP2*, a clade of six AP2 domain-containing transcription factors (*TOE1*, *TOE2*, *TOE3*, *SMZ*, and *SNZ*) comprises the predicted target set of miR172. We previously observed that the quadruple mutant, *toe1 toe2 smz snz*, flowered significantly earlier than did Col-0, *toe1*, or *toe1 toe2* double mutants (Mathieu et al., 2009). This quadruple mutant, however, did not flower as early as 35S:miR172 (Aukerman and Sakai, 2003; Chen, 2004), suggesting that there might exist further functional redundancy among the miR172 targets. Furthermore, as *AP2* has a clear flowering time phenotype and *TOE3* is a top direct regulatory target of the AP2-clade member *SMZ* (Mathieu et al., 2009), we were interested in observing the effect of a full clade, hexuple mutant loss of function.

To ensure that this suite of six genes constitutes the entire functional module of miR172 effectors, we combined a quadruple *toe1 toe2 smz snz* mutant with *toe3-1* and *ap2-12* to create a hexuple mutant miR172 target line that carries lesions in all six loci. Flowering with only 2.1 ± 0.1 rosette leaves, this hexuple mutant was significantly earlier than either Col-0 (10.4 ± 0.4 rosette leaves) or the quadruple mutant (4.9 ± 0.3 rosette leaves; Figure 2, Table 1) and phenocopied the 35S:miR172 plants very closely, which flowered after producing 2.4 ± 0.2 rosette leaves. For the quadruple, hexuple, and the miR172 overexpressor, total leaf numbers were much lower than in Col-0, but the number of leaves produced during the reproductive transition, or cauline leaves, actually increased to similar levels in both the hexuple mutant and miR172 overexpressor relative to the wild type. This points to a disconnect in this clade's function before and after the transition from vegetative growth to reproductive growth and flowering.

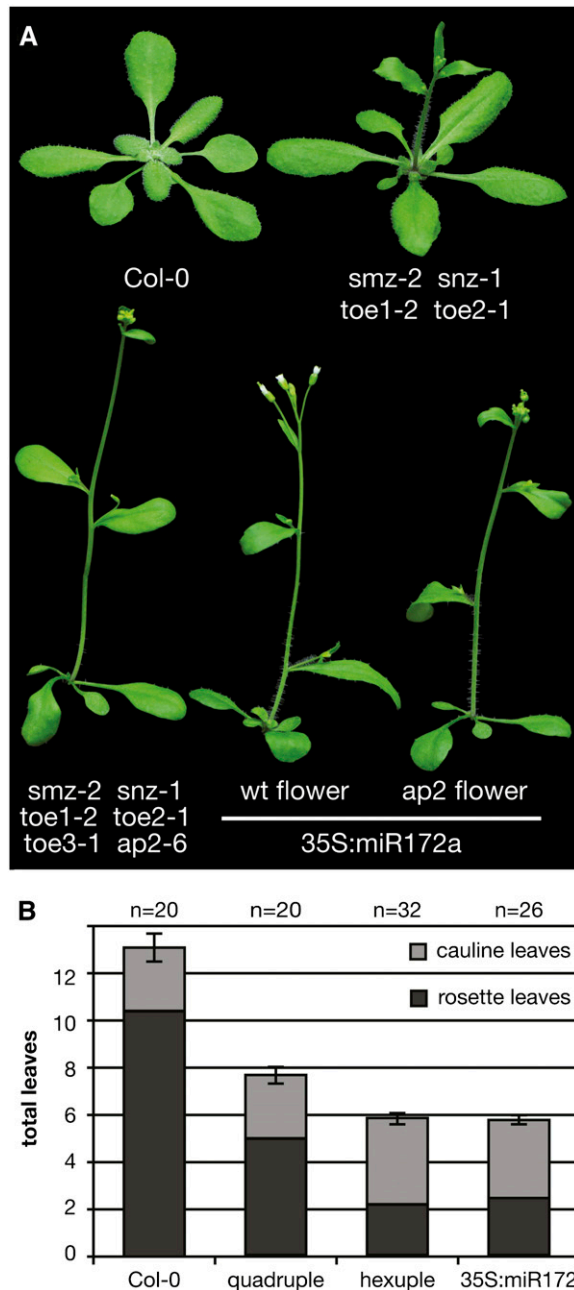


Figure 2. The Hexuple AP2-Like miR172 Mutant Recapitulates the miR172 Overexpressor.

(A) miR172 target clade quadruple (*smz-2 snz-1 toe1-2 toe2-1*) mutant, hexuple (*smz-2 snz-1 toe1-2 toe2-1 toe3-1 ap2-6*) mutant, and 35S: *miR172a* plants flower earlier than Col-0 control plants.

(B) Cauline (gray) and rosette (black) leaves to flower in mutants pictured in (A). All hexuple mutant plants and >75% of 35S: *miR172* plants exhibited the AP2 floral homeotic phenotype (i.e., lack petals). Plants were grown in long days. Error bars indicate 2xSEM of the total leaf number.

An earlier developmental phase occurring just before the transition to flowering, the juvenile to adult phase change, was also perturbed in the hexuple mutant. A hallmark of the transition from vegetative to reproductive phase in *Arabidopsis* is the appearance of trichomes on the abaxial (lower) leaf surface. In the hexuple mutants, this transition in trichome distribution was precocious. The hexuple mutants also displayed floral homeotic transformations typical of *ap2* mutants. Finally, stigmatic papillae were occasionally evident on the tips of rosette leaves, similar to what has been observed in cauline leaves in 35S:miR172 overexpressors (see Supplemental Figure 2 online; Chen, 2004), suggesting derepression of reproductive transition genes in the leaves. Consistent with this, we observed strong induction of *AG* mRNA and that of its paralogs *SHATTERPROOF1* (*AGL1; SHP1*), *SHATTERPROOF2* (*AGL5; SHP2*), and *SEEDSTICK* (*AGL11; STK*) in the leaves of the hexuple mutant by qRT-PCR (see Supplemental Figure 2 online).

Genome-Wide Identification of AP2 Binding Sites

To understand better the mechanism of AP2-mediated repression of the reproductive transition, we mapped the genome-wide binding profile of AP2 by performing chromatin immunoprecipitation coupled to ultra-high-throughput deep sequencing (ChIP-seq) and also performed inducible gene expression studies.

Based on genetic studies (Bowman et al., 1991; Drews et al., 1991), AP2 has been shown to repress *AG* expression most likely through multiple elements in the second intron (Bomblies et al., 1999; Deyholos and Sieburth, 2000). Hypothesizing that the mechanism underlying this repression might be direct chromatin binding, we tested raw technical and biological replicate ChIP samples by qPCR for enrichment of *AG* intron binding. All technical and biological replicates tested exhibited greatly enriched levels of binding at the *AG* intron, but not for two negative control regions flanking the *AG* locus (Figure 3). Independent confirmation ChIP experiments of a different mutant line, *ap2-2*, were performed with the same antibody with similar results (T. Dinh and X. Chen, unpublished data). As all pull downs exhibited enriched binding to *AG*, we processed two biological replicates by standard Illumina ChIP-seq library generation protocols to create single read libraries and sequenced them on an Illumina Genome Analyzer GAI.

Table 1. Flowering Time of Hexuple and Quadruple AP2-Like miR172 Target Mutants and miR172 Overexpressor Plants

(23°C, LD)	Rosette Leaves	Cauline Leaves	Total Leaves	2xSEM	Range	<i>n</i>
Col-0	10.4	2.7	13.1	0.6	11 - 16	20
<i>smz-2 snz-1 toe1-2 toe2-1</i>	4.9	2.7	7.6	0.2	7 - 9	20
<i>smz-2 snz-1 toe1-2 toe2-1 toe3-1 ap2-6</i>	2.1	3.7	5.8	0.2	5 - 7	32
35S: <i>miR172, T1</i>	2.4	3.3	5.7	0.3	5 - 7	26

For each genotype, the mean of the total leaf number, the deviation from the mean (2× the standard error of the mean), the range of values found for each genotype, and the number of plants examined are given.

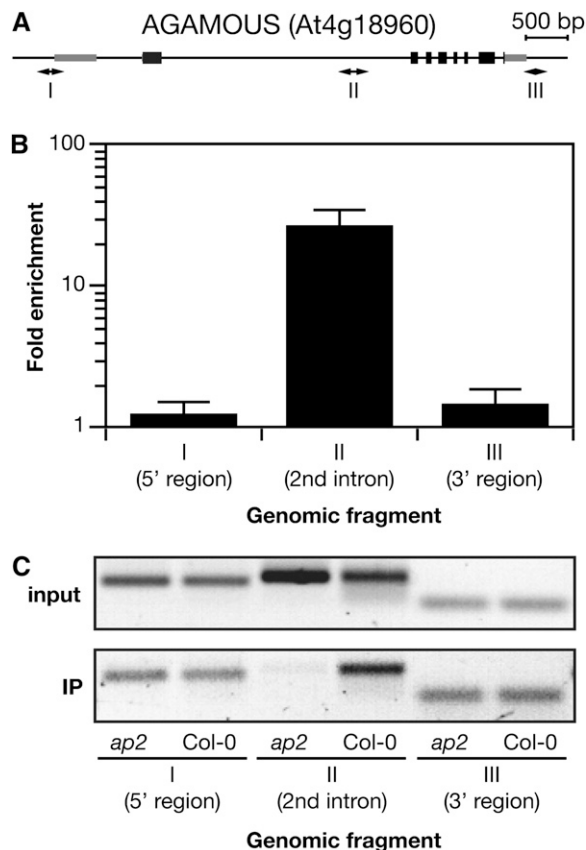


Figure 3. AP2 Binds Directly to the Second Intron of AG.

(A) ChIP-qPCR. AG locus pictured with ChIP amplicons I, II, and III.
(B) qPCR analysis of triplicate biological replicate samples for binding enrichment of AP2 in the AG second intron. Replicates from independent experiments were measured to produce mean and 2xSEM for regions mapped in **(A)**.
(C) Abundance of one biological replicate of the PCR products used to create **(B)**. PCR product for input (top) and immunoprecipitated (bottom) DNA is shown for Col-0 and *ap2-12* for the three amplicons (I, II, and III) tiling the AG locus.

After filtering for read quality and nonrepetitive mappability, between 5.2 and 14.2 million sequencing reads were uniquely mapped to the TAIR9 genome per sample (see Supplemental Table 2 online). We used SHORE (Ossowski et al., 2008) for mapping to the genome and performed enrichment analyses with an algorithm we developed specifically for *Arabidopsis* ChIP-seq peak calling. High confidence binding sites were identified by determining the overlap between highly significantly (false discovery rate [FDR] < 10^{-10}) enriched bound regions in both biological replicates that also were enriched by a per base excess enrichment cutoff (see Methods for details). A total of 2275 regions in the nuclear genome were found to be significantly enriched in both independent biological replicates by these stringent criteria (see Supplemental Data Set 1 online). To ensure that our algorithm performed at least as well as published peak detection methods, we analyzed our AP2 data set using CisGenome (Ji et al., 2008) and compared the results to those

obtained using our algorithm. Whereas CisGenome identified most of the targets that our algorithm did (2158 of 2275 at FDR < 0.01 in CisGenome), our script allowed us more transparency over the peak calling, so we continued analysis with this algorithm. The average width of these 2275 regions was 248 bp (Table 2).

Genome-Wide Physical Distribution and Functional Classification of Bound Loci

Of the bound regions flanking genes, more were associated with regions <1 kb upstream of transcription start sites or 5' UTRs than with the regions <1 kb downstream of transcription end sites or 3' UTRs (see Supplemental Figure 3 online), similar to what has been observed for other *Arabidopsis* transcription factors, such as SEP3 (Kaufmann et al., 2009) or AGL15 (Zheng et al., 2009). Of those top 200 bound regions, 66 were located <1 kb upstream of a transcription start site. Several enrichments were evident for particular gene ontology (GO) categories among the 1780 bound loci for which GO assignments exist. Genes associated with organ development (GO:0048513) and transcription regulator activity (GO:0030528) were significantly over-represented at a FDR $P < 0.0005$ among the list of AP2-bound loci, indicating functional specificity of target binding. Among the other biological processes found to be significantly ($P < 0.01$) over-represented were shoot development (GO:0048367), shoot morphogenesis (GO:0010016), flower development (GO:0009908), transcription (GO:0006350), and DNA binding (GO:0003677).

AP2 Directly Binds Key Flowering Time Loci

GO category enrichment indicated that AP2 occupies many loci involved in shoot development and morphogenesis in addition to floral development, consistent with the pleiotropic phenotypes of *ap2* mutants. We hypothesized, however, that its role in the control of flowering time might involve loci just upstream of these well-described downstream floral organ development processes. Loci marking the transition to flowering, *AP1* and *SOC1*, were bound with high confidence (FDR < 10^{-10}) in both biological replicates, along with the floral organ identity genes *SEPALLATA3* (*SEP3*) and *AG* (Figures 4A to 4D). The AP2-bound regions were all positioned in the 5' sequences <1.6 kb upstream of the transcription start sites for *SOC1*, *AP1*, and *SEP3*; the region in *AG*, however, was in the 3' end of the second intron (Figure 4A). The specific region bound in the *AG* intron corresponded closely with our ChIP qPCR (Figure 3), confirming those results (see Supplemental Figure 4 online).

Interestingly, AP2 also directly bound to its own genomic locus and to those of clade members *TOE3*, *SMZ*, *TOE1*, and *SNZ*, for a total of five of the six AP2-like miR172 targets, consistent with the previously observed feedback regulation of AP2 (Schwab et al., 2005). In fact, the *TOE3*, *AP2*, *SOC1*, and *SEP3* loci each contained multiple AP2-bound regions (Figures 4B, 4C, and 4E). The *SMZ* locus also had two high ranking regions <1 kb upstream of its transcription start site. Interestingly, another floral repressor, the MADS domain protein AGL18 (Adamczyk et al., 2007) was the nearest locus to multiple AP2-bound sites.

Table 2. Summary Characteristics of AP2 Peak Regions as Determined by ChIP-Seq

Description	Value
Average peak region width (bases)	248
Number of bound regions at FDR < 10 ⁻¹⁰ + per base excess >0.25	2275
Peaks <4 kb upstream from TSS or <2 kb downstream from TES	2247

TSS, transcription start site; TES, transcription end site.

Gene Expression Changes in Response to AP2 Loss of Function

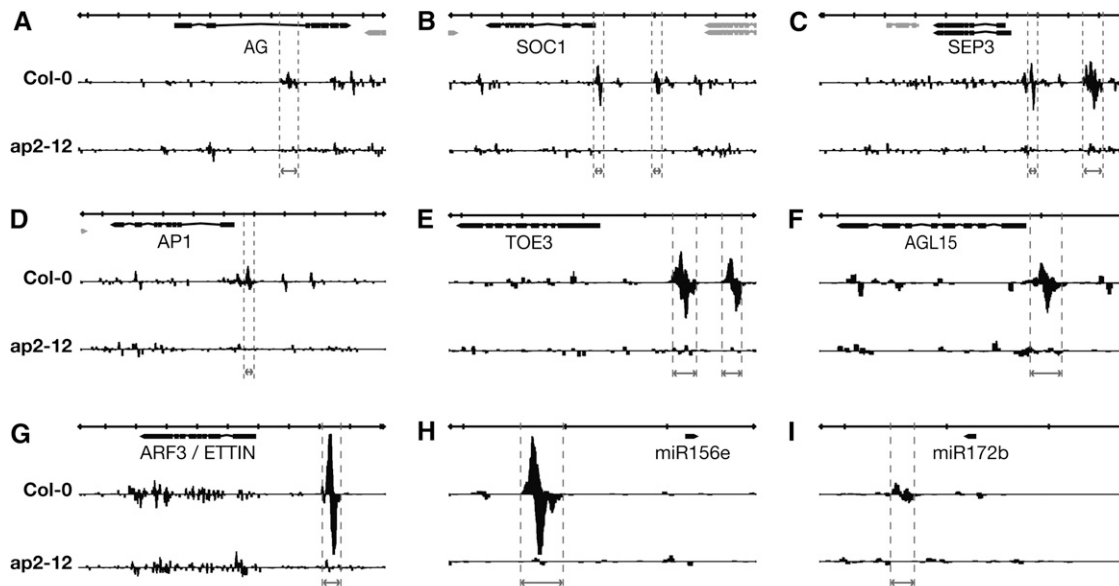
To understand the global effects of AP2 on the shoot transcriptome and to identify direct targets for which AP2 DNA binding may have an effect on transcript levels, we analyzed expression data from the inflorescences of *ap2-6* mutants and Col-0 from the AtGenExpress developmental gene expression atlas (Schmid et al., 2005) (see Supplemental Data Set 2 online). As expected, AP2 RNA levels were significantly (RankProducts, percentage false positives [pfp] < 0.05) downregulated in *ap2* mutant plants (Figure 5A). Consistent with its highly connected gene regulatory role and repressor function, 198 nuclear-encoded genes were upregulated and 162 were downregulated in *ap2* mutant inflorescences (pfp < 0.01) relative to the wild type.

Elevated levels of several transcripts influencing flowering time were detected in *ap2* mutants. While levels of *CONSTANS*,

FT, and *TWIN SISTER OF FT* transcripts were not significantly different from the wild type, downstream of these genes, *SOC1*, *FRUITFULL (FUL)*, and *AG* levels were significantly (pfp < 0.01) elevated in the *ap2* mutant (Figure 5A), consistent with AP2 repressing these genes.

To confirm the effect of *ap2* loss of function in the native context at the time the commitment to flowering is made but before reproductive structures are morphologically evident, we measured the mRNA abundance of two key redundant floral activators, *SOC1* and *FUL*, by qRT-PCR on the aerial parts of 8-d-old LD-grown *ap2-12* seedlings. Similar to the array data from bolting *ap2-6* inflorescences (Figure 5A), both *SOC1* and *FUL* transcript levels were upregulated in this early transition *ap2* mutant seedling tissue (Figure 6B).

Extensive feedback regulation has been observed in the clade of AP2-like miR172 targets, and we accordingly observed significantly upregulated *TOE1* and *TOE3* transcript levels in the *ap2* mutants (Figure 5A). Of the transcripts downregulated in the *ap2* mutant, only one stood out in regard to flowering: another floral repressor, *TFL1*, was significantly (pfp < 0.01) downregulated in the *ap2* mutant (Figure 5A). Finally, as lipid transfer proteins have been implicated in *TFL1* function (Sohn et al., 2007) and in pollen tube growth (Chae et al., 2009), we note that the four most upregulated transcripts in *ap2* plants encoded lipid transfer proteins. Two of these four lipid transfer protein loci are bound by AP2, but the *TFL1* locus is not. It has recently been reported, however, that AP1, which we identify as a direct transcriptional target of AP2, itself directly binds the *TFL1* locus (Kaufmann et al., 2010).

**Figure 4.** ChIP-Seq Reveals Direct AP2 Targets.

GBrowse traces of mapped ChIP-seq reads. In each panel, the top row indicates scale, with bold vertical lines indicating 1-kb increments. Gene models are shown under the scale bar, and single biological samples are pictured below. Forward reads are mapped above each line and reverse reads below. Regions adjacent to or inside introns of *AG*, *SOC1*, *SEP3*, *AP1*, *TOE3*, *AGL15*, *ARF3*, miR156, and miR172 are bound with high confidence (FDR < 10⁻¹⁰) in both biological replicates versus control samples in the *ap2* mutant line. Vertical dotted lines delimit the position of the peak regions.

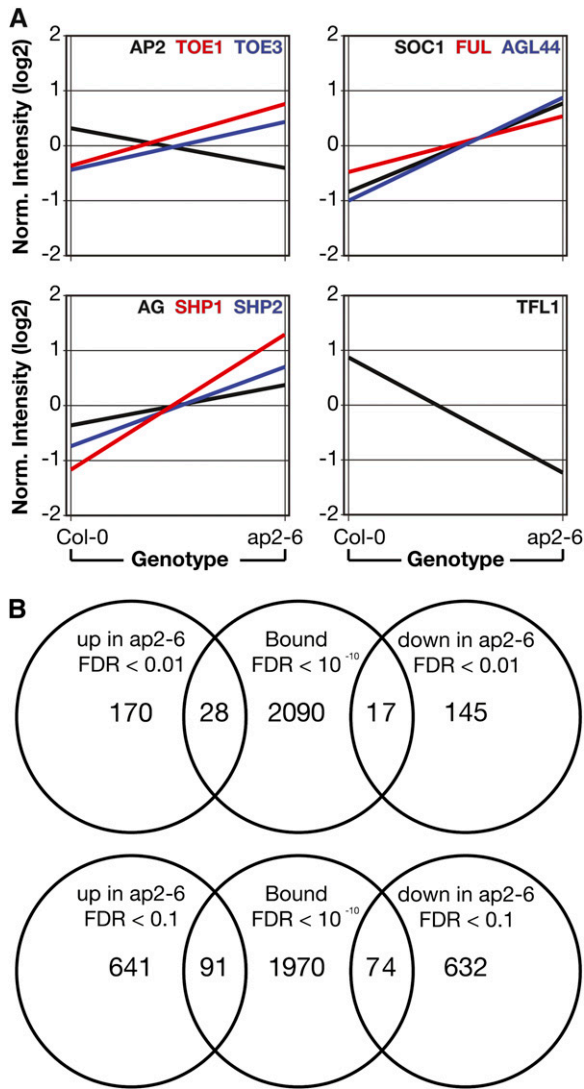


Figure 5. Overlap of Genome-Wide Binding and Expression.

(A) Gene expression changes in *ap2-6* inflorescences as determined by Affymetrix microarray analysis.

(B) Overlap of loci bound by AP2 (determined by ChIP-seq) with transcripts differentially expressed in *ap2* mutants (from **[A]**). Top Venn diagram indicates transcripts changed at RankProducts $p < 0.01$, and bottom Venn diagram indicates transcripts changed at RankProducts $p < 0.1$.

Regulators of the Floral Transition and Floral Development Are Direct AP2 Targets

Having identified genome-wide AP2 binding sites and surveyed the transcriptome for genes that were differentially expressed in *ap2* mutant plants, we sought to determine whether there was overlap between these data sets, which would indicate direct targets for AP2 (Figure 5B). In all, 91 loci were directly bound by AP2 and also upregulated in the *ap2* mutant (binding FDR 10⁻¹⁰; expression FDR < 0.1; see Supplemental Data Set 3 online), suggesting that AP2 directly represses these genes. Seventy-

four loci were directly bound by AP2 but downregulated in the *ap2* mutant, suggesting the possibility that AP2 might also function as a positive regulator of transcription.

In surveying the set of these directly bound and regulated loci, we observed a synergistic effect. Particular GO categories, which were somewhat enriched in the list of bound genes and in the list of misregulated genes, were much more enriched in the overlap list of genes that were both bound and regulated by AP2 (see Supplemental Figure 5 online). Biological processes implicated in gynoecium, flower, carpel, floral whorl, and floral organ development all demonstrated this trend, as did the molecular functions transcription regulator activity, DNA binding, and regulation of transcription.

Several genes that play central roles in flowering and floral organ identity were among these AP2 direct targets, indicating

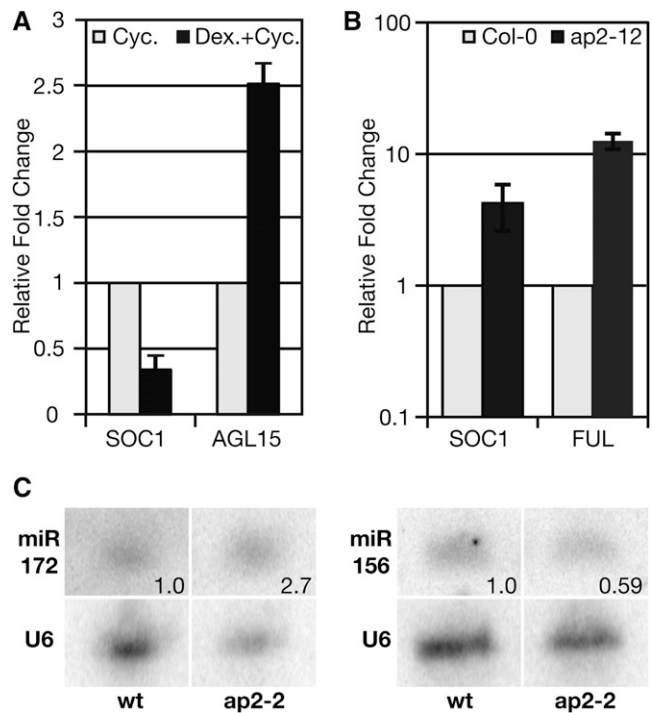


Figure 6. AP2 Activates and Directly Represses Flowering Time Genes.

(A) Direct activation of *AGL15* or repression of *SOC1* was assayed by qRT-PCR in *35S:AP2m3-GR* seedlings grown for eight LDs and treated with 10 μM CYC in the presence (black) or absence (gray) of 10 μM DEX. Data shown are representative of one biological replicate and three technical replicates from which SD was calculated. These data are representative of quadruplicate biological replicates, all of which showed similar results.

(B) *SOC1* and *FUL* transcripts are upregulated in *ap2* mutants undergoing the transition to flowering. Error bars indicate SD of triplicate biological replicates.

(C) miR172 and miR156 participate in a complex feedback loop with AP2. Small RNA gel blotting to detect miR172 and miR156 levels in wild-type versus *ap2-2* dissected inflorescence tissue. The number on the gel images indicates relative abundance of the small RNAs normalized to the loading control (U6). This assay was repeated twice with similar results.

that the influence of *AP2* on flowering time is quite direct. These include the MADS domain genes *SOC1*, *AG*, and its paralogs *SHP1* and *SHP2*, all of which were upregulated in the *ap2* mutant and bound by AP2 (binding FDR 10^{-10} ; expression FDR < 0.05). Another MADS domain gene that was bound by AP2 and upregulated in the *ap2* mutant is *AGL44*. This gene is strongly upregulated over the course of the floral transition but until now has not been closely associated with flowering. In addition, the AP2-like miR172 targets *TOE1* and *TOE3* and the locus encoding the DELLA protein *RGA-like1* were directly bound and upregulated by AP2. Of the 74 directly bound loci whose transcript levels were downregulated ($p < 0.1$) in the *ap2* mutant, only one, *AGL15*, stood out in relation to flowering time (binding FDR 10^{-10} ; expression FDR = 0.07). Interestingly, this gene was recently shown to act redundantly with *AGL18* as a repressor of flowering in a daylength-independent manner, like *AP2* (Adamczyk et al., 2007).

The combined analysis of genome-wide direct binding and global gene expression changes indicates that AP2 regulates flowering by modulating the expression of a range of known flowering time and organ identity genes. Furthermore, the expression of other floral repressors is dependent on AP2, with one, *AGL15*, both directly bound by AP2 (Figure 4F) and downregulated in the *ap2* mutant. This raises the possibility that AP2 may act not only as a direct repressor but also as a bifunctional transcriptional regulator that either directly activates or directly represses the transcription of particular target genes.

Inducible AP2 Confirms Direct Targets and a Bifunctional Molecular Role

To explore whether these AP2 regulatory interactions were direct or indirect, we employed an inducible expression system. We expressed a translational fusion of AP2m3 (a miR172-resistant version of AP2) (Chen, 2004) to the hormone binding domain of the rat glucocorticoid (GR) receptor under the control of a constitutive promoter, the cauliflower mosaic virus 35S. Treatment with the GR ligand dexamethasone (DEX) allows AP2m3-GR entry to the nucleus, while administration of cycloheximide (CYC) inhibits protein synthesis, allowing the detection of direct AP2 transcriptional targets by quantitative PCR. The functionality of AP2m3-GR was revealed by the typical AP2m3 floral phenotype and the late flowering induced by DEX treatment (see Supplemental Figure 6 online; Chen, 2004). Using this system, we observed significant downregulation of *SOC1* transcript levels in response to DEX treatment in the absence of protein synthesis, indicating that AP2 directly represses the transcription of *SOC1* in 8-d-old seedlings when the decision to flower is being made (Figure 6A). By contrast, we observed significant upregulation of the directly bound floral repressor *AGL15* in response to DEX treatment, confirming that AP2 can act also as a direct transcriptional activator (Figures 6A and 4F).

AP2 Participates in a Feedback Loop with Its Regulators miR172 and miR156

We observed that several of the highest confidence AP2 binding sites from the ChIP-seq experiment were associated with micro-

RNAs that regulate developmental processes, such as flowering and phase transition. The most striking of these was the #2 genome-wide peak (as rank sum of biological replicate rankings), which was centered immediately upstream of miR156e (Figure 4H). This microRNA affects the juvenile-to-adult phase transition (Wu et al., 2009) and an endogenous flowering pathway (Wang et al., 2009) by negatively regulating the expression of miR172b (Wu et al., 2009). This latter microRNA, miR172b, was another high-confidence target of AP2 (Figure 4I), making these two microRNAs the highest-ranking microRNAs in the AP2 target list. These interwoven connections between AP2 and the two microRNAs that regulate it suggest a highly buffered regulatory network controlling the closely related developmental processes underlying phase transition and flowering time.

We sought to determine whether the expression of these microRNAs is changed as a result of changes in AP2 expression, which would indicate that this binding has a functional consequence. We therefore performed small RNA gel blots on inflorescence tissue from *ap2-2* mutants and compared the abundance of these microRNA families to that in wild-type plants. Levels of miR172 in *ap2* mutants were 270% of those in the wild type, while levels of miR156 in *ap2* mutants were 59% of those in the wild type (Figure 6C), indicating that AP2 not only binds to but also negatively regulates miR172 and positively regulates miR156. Thus, multiple lines of evidence (ChIP-seq and gene expression changes in response to AP2) point to this selective and direct positive and negative regulation of developmental microRNAs by AP2.

AP2 Target Binding during AP2-Mediated Floral Repression in Leaves

Based on the well-known *ap2* floral homeotic phenotype, we initially expected to observe a genetic role for AP2 primarily in the regulation of loci involved in early floral whorl development. Surprisingly, however, AP2 bound to numerous loci influencing the transition from vegetative growth to flowering, even in the developing inflorescence. We therefore followed these data to investigate whether active AP2-mediated floral repression resulted in binding to the same loci. Because several of the members of the AP2-like miR172 target clade, including AP2 itself, are expressed in vegetative apices and in leaves (Okamoto et al., 1997; Schwab et al., 2005; see Supplemental Figure 7 online), we reasoned that AP2 may repress flowering by mechanisms similar to the closely related SMZ (Mathieu et al., 2009). We therefore employed a strategy that would provide direct comparisons to the previous SMZ ChIP-chip experiments (Mathieu et al., 2009), while also assaying AP2 binding during active repression of flowering by AP2 with an independent antibody to corroborate our native inflorescence ChIP-seq.

We prepared a translational fusion of an miR172 targeting-resistant version of AP2 (*rAP2*) (Schwab et al., 2005) to green fluorescent protein (GFP) driven by the 35S promoter. The *rAP2* transcript carries silent mutations within the miR172 target site. An important advantage of this strategy is that it allows the demonstration of AP2 binding to target loci during the strong floral repression of 35S:*rAP2*, which results in a very clear floral repression phenotype directly attributable to *rAP2* function

(Chen, 2004). For a genome-wide view, we performed ChIP followed by hybridization to Affymetrix genome tiling arrays (ChIP-chip). This AP2-GFP fusion protein retains activity, as evidenced by extremely late flowering and crinkly leaves, which recapitulates the 35S:AP2m3 phenotype (Chen, 2004). As a negative control for 35S:AP2-GFP plants, we used a nuclear-localized GFP expressed from the same promoter. Eight tiling arrays were hybridized with material from two biological replicates of each genotype and two technical ChIP replicates of each biologically independent sample. This also serves as an independent corroboration of our ChIP-seq experiment employing an anti-AP2 antibody and native expression.

By ChIP-chip of the leaves with an independent GFP antibody, we detected high confidence binding to many of the same target loci that we found by native ChIP-seq of inflorescence tissue, especially those among the top targets. The same loci encoding *ARF3/ETTIN*, *SOC1*, *SEP3*, *AP1*, *TOE1*, *TOE3*, *SMZ*, *SNZ*, *RGA1*, *AGL15*, and *AGL44* were all bound with an FDR < 0.05 (CisGenome default analysis as in Mathieu et al., 2009; see Supplemental Figure 8 and Supplemental Data Set 4 online). However, we could not detect any trace of binding to the *AG* intron in the leaf tissues (see Supplemental Figure 9 online), despite hybridizing multiple independent samples. This may suggest that the native ChIP-seq experiment can detect *AG* binding because of the presence of particular cofactors at the apex that were not available in the tissues assayed by ChIP-chip. For the other loci listed above (and others), however, strong binding was detected in both tissues (see Supplemental Figures 9C and 9D online). Furthermore, expression analysis in the inducible AP2m3-GR line during the time the commitment to flowering is made indicates that key floral genes *SOC1* and *AGL15* (Figure 6A) are directly regulated by AP2. qPCR expression analyses on the *ap2-12* loss-of-function line (Figure 6B) show that the functionally redundant *SOC1* and *FUL* are negatively regulated by AP2 when the decision to flower is being made. Taken together, these data indicate that AP2 can influence the expression of these targets during early vegetative growth, in inflorescences, and also when actively repressing flowering in an overexpression context.

Whereas nearly all of the major flowering-related genes were similarly enriched in leaf ChIP-chip as in inflorescence ChIP-seq experiments, surprisingly, we did not detect binding to miR172b or miR156e in the leaf tissue by ChIP-chip. This is not likely due to a difference in sensitivity between these methods, as both loci are well bound in inflorescence tissue, with miR156e a genome-wide top target (Figure 4H; see Supplemental Data Set 1 online). Because AP2-dependent expression of these transcripts was confirmed by expression analysis in inflorescence tissue (Figure 6C), we conclude instead that these different tissues may have contrasting chromatin accessibility profiles, possibly accounting for this striking difference. Findings such as these suggest the need for tissue-specific chromatin accessibility surveys to interpret better the data generated in genome-wide ChIP experiments. This would also better distinguish whether different levels of binding for a particular locus occur in different tissues as a result of the differential presence of particular transcriptional cofactors or contrasting epigenetic regulation.

DISCUSSION

Considered generally a transcriptional repressor, AP2 is a versatile protein, with effects not only on flowering time, but also on ovule and seed coat development, floral organ morphogenesis, and the maintenance of the stem cell niche. The degree of pleiotropy exhibited by *ap2* mutants is unusual. This is perhaps more surprising given that AP2 is a member of a group of closely related targets of a major developmental microRNA, miR172. While this pleiotropy fits the general theme of floral repressor phenotypes (Poureau et al., 2004; Del Olmo et al., 2009), why is it so clearly associated with AP2 and not the other AP2-like miR172 targets, which are partially redundant with AP2 and one another, at least in the governance of flowering time? How the phenotypic output and function of these targets is coordinated is currently not well understood, but elucidating their direct transcriptional target repertoires promises to clarify better this functional divergence.

We set out to address the following question: How does AP2 suppress flowering? Clearly, AP2 and the other members of the miR172 target clade share some direct network connections to achieve this end, but some findings are specific to each protein. SMZ expression, for example, is relatively concentrated in the young seedling as evidenced by β -glucuronidase staining (Mathieu et al., 2009), where it directly represses *FT* transcription. AP2, on the other hand, has been previously shown to act at the shoot apical meristem (Wurschum et al., 2006). Similarly, we found AP2 to repress directly the reproductive genes *AG* and *SOC1* at the shoot apex, while it did not repress *FT* in leaves, as assayed in both tissues by genome-wide, direct chromatin binding approaches. This indicates that AP2 primarily acts as a flowering time integrator at the shoot apex. AP2, however, also directly bound the *SOC1* and *FUL* loci in our ChIP-chip experiment, and consistent with this, *SOC1* and *FUL* transcript levels were upregulated in the aerial tissues of *ap2* mutants. We also observed this upregulation in *ap2* mutant inflorescence arrays. The functional redundancy of *SOC1* and *FUL* has been shown to affect dramatically both flowering time and meristem determinacy (Melzer et al., 2008). Another of the best bound AP2 direct targets was *ARF3/ETTIN* (Figure 4G). *ARF3/ETTIN* is involved in floral organ identity and the promotion of adult leaf traits (Sessions et al., 1997; Fahlgren et al., 2006; Hunter et al., 2006) and is therefore a potential mediator of the precocious phase change observed in our AP2 clade hexuple mutant. Overall, the complex pleiotropy of AP2, and the interplay of a gene traditionally considered a floral organ specificity factor with flowering time, fits with an emerging picture of shared function between floral patterning and flowering time genes more generally (Liu et al., 2009).

Perhaps the most well-known function for AP2 is as an A-class floral homeotic gene, promoting sepal and petal identity and opposing C class function (Bowman et al., 1991; Drews et al., 1991; Bomblies et al., 1999). Here, we observe that AP2 directly targets not only the C locus exemplum *AG* but also its ancient paralogs the *PLE* genes (Kramer et al., 2004; Causier et al., 2005), represented in *Arabidopsis* by *SHP1* and *SHP2*. Interestingly, targeting is present, although these lineages have undergone subfunctionalization since divergence: while *AG* is involved in

floral meristem determinacy, carpel and stamen identity, and ovule development (Bowman et al., 1989), *SHP1* and *SHP2* are more functionally constrained, contributing to ovule identity and influencing particular tissue types in fruit development (Liljegren et al., 2000; Pinyopich et al., 2003). Whether *AP2* orthologs in other species might exhibit targeting of the *AG* and *PLE* lineages would be an interesting question to address. We hope that this data set will facilitate further analysis of this question and, more broadly, precisely how *AP2* orchestrates both flowering time and gynoecium development.

One of the most unexpected findings of this study was that *AP2* can function not only as a direct repressor but also as a transcriptional activator of divergent gene classes that share a common function: one, a transcription factor that represses flowering, and the other, a microRNA that also represses flowering. Direct activation of the floral repressor *AGL15* is evidenced by inducible gene expression assays in the absence of protein synthesis and direct chromatin binding by ChIP-seq. Functionally, this relationship makes sense given the floral repressor roles of all three genes. The second instance we demonstrate of direct bifunctional activation and repression by *AP2* is its direct regulation of its own regulators, *miR156* and *miR172*. Again, in this case, the direction of regulation is logical: *AP2* directly promotes the expression of the floral repressor *miR156*, which, in turn represses the repressor of *AP2*, *miR172*, a floral activator (Figure 7). That this repression is even evident in microRNA abundance is all the more significant, as there are multiple family members of each of the two microRNAs (*miR156a-h* and *miR172a-e*), but only one family member of each microRNA is bound by *AP2*, *miR172b*, and *miR156e*. Thus, while evident, the expression difference is by necessity only moderately changed in the *ap2* mutant due to the redundant activity of other microRNA family members.

While the observation that *AP2* influences flowering time redundantly with its fellow *miR172* targets was no great surprise, we did not anticipate that lesions in *AP2* alone would have such substantial effects, with the mutant flowering 23 leaves earlier than controls in short days. This incomplete redundancy among the *AP2*-like *miR172* targets suggests a diversity of mechanisms by which family members fine-tune flowering time, making this *miR172* target node an interesting model for discrete gene regulatory modules in complex organisms. The eventual recapitulation of the 35S:*miR172* phenotype in the hexuple mutant demonstrates at the phenotypic level that these six genes, *AP2*, *SMZ*, *SNZ*, *TOE1*, *TOE2*, and *TOE3*, constitute the entire complement of effectors of this microRNA, which is consistent with the absence of additional predicted *miR172* targets involved in the floral transition.

The recent advent of whole-genome approaches to the question of direct transcriptional interactions can facilitate new insights into how transcription factors coordinate their actions across the genome. We recently mapped the genome-wide binding profile of *SMZ* (Mathieu et al., 2009). Thus, we now have an opportunity to compare the direct target repertoires of these family members. Indeed, many high confidence flowering loci were targeted by both the *AP2* and *SMZ* proteins: *TOE3* was bound with the highest confidence values, and the loci *SMZ*, *SNZ*, *AP2*, *AP1*, *SOC1*, and *SEP3* were also bound by both *SMZ*

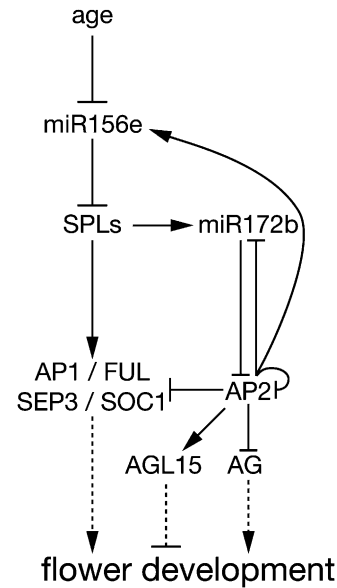


Figure 7. Salient *AP2* Direct Network Connections to Flowering Time and Organ Development Genes.

AP2 participates in multiple feedback loops by directly binding flowering time loci and modulating their expression in logical, reinforcing circuits. *AP2* directly represses the expression of flowering promoting transcripts *AP1*, *FUL*, *SEP3*, and *SOC1* by binding to their genomic loci. At the same time, *AP2* directly promotes the expression of *miR156e*, which represses the floral transition by repressing the *SPLs*. Additional, dual feedback loops via the repressor of *AP2*, *miR172b*, are evident, with *AP2* directly repressing *miR172b* and also reinforcing this direct action on *miR172b* through increased *miR156e* expression. Finally, *AP2* directly promotes the expression of the unrelated MADS domain floral repressor, *AGL15*, while directly repressing the expression of *AG*, a key MADS domain floral identity gene.

and *AP2*. Other loci encoding transcription factors not obviously involved in flowering, such as *TOPLESS RELATED1* (*TPR1*), *TPR2*, and *AGL44* (*ANR1*) were bound by both transcription factors, in addition to 92 other protein coding loci (see Supplemental Table 3 online). The significance of the regulation of these genes by *AP2* and *SMZ* is currently unknown but indicates additional functions that may have been obscured by the extreme redundancy in this clade. On a genome-wide scale, *AP2* did bind to many of the same loci as *SMZ* did: Of the 372 protein coding gene loci most closely associated with an *SMZ*-bound region, over 27% (102) also are the nearest annotated locus to a high confidence *AP2*-bound region, pointing to both shared function and divergence.

Because the *AP2* ChIP-seq experiment reported here was more sensitive than the *SMZ* ChIP-chip experiment, we can compare results only unidirectionally; an absence from the *SMZ* data set and presence in the *AP2* data set (as in the case of *AG*, for example) cannot necessarily be interpreted that *AP2* targets a locus that *SMZ* definitely does not. We can, however, make inferences in the reverse direction. Loci that we observed in the less sensitive *SMZ* ChIP-chip experiment that we did not observe in the more sensitive *AP2* ChIP-seq experiment are

almost certainly meaningful differences. Indeed, a divergence in target repertoire is clearly evident: the flowering time loci *FT* and *TEM1* were among the top 434 genomic regions bound by SMZ (FDR < 0.05) but not the top 2275 genomic regions bound by AP2 in inflorescences (FDR < 10^{-10}). However, because the 35S:rAP2-GFP ChIP-chip experiment was performed on leaf tissue from the same promoter and assay as the SMZ experiment, comparisons are valid. In contrast with the native AP2 ChIP-seq experiments on inflorescence tissue, we failed to detect binding to *AG* in leaf tissue but did detect high confidence binding of AP2 to the *TEM1* locus in leaf tissue, consistent with the expression and functional domains of these direct targets. Thus, while AP2 and SMZ are partially redundant, sharing some direct transcriptional targets, each has a distinct repertoire that may differ from tissue to tissue.

Understanding the level of complexity inherent in developmental gene regulatory networks has only just begun, as the ability to analyze genome-wide binding profiles of key transcription factors is in its infancy. A handful of studies have reported binding profiles for the transcription factors *SEP3*, *AGL15*, *AP1*, *SMZ*, and now, *AP2*. Results of these studies indicate widespread interaction between AP2-like and MADS domain transcription factors, a pattern that we will surely see extended to many transcription factor classes. More generally, they indicate an unexpected level of complexity in the interactions of these transcription factors with one another and their targets. Furthermore, it may be expected that such studies will likely illuminate new aspects of transcriptional regulation: for example, transcription factors generally considered to be solely activators or repressors may be discovered to have more subtle and particular direct effects on the transcription of a diversity of target genes. The mechanisms underlying these diverse functions may only be speculated upon here but may indicate the activity of cofactors that may help control the transcriptional activating or suppressing roles, as has been indicated for other transcription factors.

METHODS

Sequences of oligonucleotide primers used in this work are given in Supplemental Table 4 online.

Plasmid Construction

The cDNA of a miR172-resistant version of AP2, AP2m3 (Chen, 2004), was amplified by PCR using oligos AP2ProKPNF and AP2cDNANOTR using *pAP2:AP2m3* (Zhao et al., 2007) as a template, digested by *KpnI*-*NotI*, and cloned into the pENTR1A vector (Invitrogen). A Gateway destination vector (pBI-GR-GW) containing the 35S promoter and the GR was subsequently used to generate the 35S:AP2m3-GR plasmid. To generate the 35S:rAP2-3xYFP transgenic construct, 3xYFP-NLS (Heisler et al., 2005) was cloned into a modified Gateway entry plasmid (pJL-Blue) in between the *attL1* and *attL2* recombination sites to create pHW100. The AP2 cDNA lacking the stop codon was released from plasmid pRS276 as an *EcoRI* (blunted)/*SpeI* fragment and cloned in front of the 3xYFP-NLS in the pJL-Blue vector to generate an entry plasmid containing the AP2-3xYFP-NLS open reading frame. Mutations rendering AP2 resistant to miR172 (Schwab et al., 2005) were introduced by site-directed mutagenesis using oligos G-1895 and G-1896 to create pHW154. For plant transformation, the entry plasmid containing the

rAP2-3xYFP-NLS open reading frame was recombined into a pGREEN-II based binary plasmid carrying the cauliflower mosaic virus 35S promoter in front of the Gateway recombination cassette (Mathieu et al., 2007) to create pHW159.

Plant Transformation and Growth

The *AP2m3-GR* construct was transformed into *Agrobacterium tumefaciens* strain GV3101 and introduced into a population segregating for *ap2* via the floral dip method. Positive transformants were selected for kanamycin resistance. *AP2m3-GR* transgenic lines with a single-locus T-DNA insertion were subsequently identified based on the 3:1 segregation ratio between kanamycin resistance to sensitivity. The 35S:rAP2-3xYFP construct was transformed into *A. tumefaciens* strain ASE, and T1 transformants were selected on kanamycin.

Plant Material

Wild-type plants were of the Col-0 accession in all experiments except in comparisons to *ap2-2*, where we used the Landsberg *erecta* accessions. All T-DNA insertion mutants used in this work are in Col-0 accession except *ap2-2*, which was in Landsberg *erecta*. *ap2-2*, *toe1-2*, *toe2-1*, *soc1-2*, *ft-10*, *co-9*, and 35S:*miR172a* have been described before (see Supplemental Table 5 online). Mutant plants were confirmed by PCR-based genotyping

Growth Conditions

All plants, except those from the GR experiments, were grown in growth chambers in a controlled environment (23°C, 65% relative humidity). Plants were raised on soil under a mixture of Cool White and Gro-Lux Wide Spectrum fluorescent lights, with a fluence rate of 125 to 175 $\mu\text{mol m}^{-2} \text{s}^{-1}$. All light bulbs were of the same age. LD is defined as 16 h light and 8 h dark and SDs as 8 h light and 16 h dark. For flowering time measurements, plants were randomized with the respective controls, and the flowering time phenotype was determined without prior knowledge of the genotype.

Total RNA Extraction and Quantitative Real-Time PCR

Total RNA was extracted from plant tissue using the Plant RNeasy kit (Qiagen) according to the manufacturer's instructions. Two micrograms of total RNA was DNase I-treated and single-stranded cDNA was synthesized using oligo(dT) and the RevertAid first strand cDNA synthesis kit (Fermentas). Quantitative real-time PCR was performed on an Opticon Continuous fluorescence detection system (MJR) using the Platinum SYBR Green qPCR Supermix-UDG (Invitrogen). Gene expression was calculated relative to β -tubulin using the $\Delta\Delta\text{CT}$ method. For qRT-PCR, all results are reported for triplicate reactions. For the GR experiments, cDNA was synthesized from total RNA isolated from chemically treated seedlings. qRT-PCR to detect *SOC1* and *AGL15* transcript levels was performed using the Bio-Rad Real-Time PCR SYBR Green Mix. Three biological replicates were performed. Oligonucleotide primers used for qRT-PCR are listed in Supplemental Table 4 online.

Microarray Expression Analysis

Analysis of inflorescence transcriptomes in *Arabidopsis thaliana ap2-6* and Col-0 plants was performed on data from the AtGenExpress data set (Schmid et al., 2005). Lists of statistically significantly expressed genes were calculated for pairwise comparisons between the two genotypes using RankProducts (version 2.6.0) implemented in R (version 2.4.0; GUI 1.17) on gcRMA (version 2.6.0) normalized expression estimates (Breitling et al., 2004; Wu et al., 2004).

Cross-Linking, Chromatin Isolation, and ChIP-Seq

The entire experiment from harvest through deep sequencing was repeated twice to produce independent biological replicates. ChIP-seq was performed with an antibody raised against the C terminus of AP2 amino acids 289 to 432 (right after the second AP2 DNA binding domain until the stop codon). Col-0 plants were used to determine binding sites in the fully native context, and *ap2-12* plants were used as negative controls for any nonspecific background antibody binding and pull down. To maximize AP2 levels, we harvested clusters of young inflorescences at the beginning of bolting, but before flowers opened, when AP2 expression is high. Briefly, clusters of just-bolting inflorescences were harvested and fixed as described previously (Gomez-Mena et al., 2005). Frozen tissue was ground, filtered three times through Miracloth (Calbiochem), and washed as described previously through buffers M1, M2, and M3 (Gomez-Mena et al., 2005). Nuclear pellets were resuspended in sonic buffer as described (1 mM PEFA BLOC SC [Roche Diagnostics] was substituted for PMSF), split into technical duplicate samples, and sonicated with a Branson sonifier at continuous pulse (output level 3) for eight rounds of 2×6 s and allowed to cool on ice between rounds. Immunoprecipitation reactions were performed by incubating chromatin with 2.5 μ L anti-rabbit AP2 antiserum overnight at 4°C as described (Gomez-Mena et al., 2005). The immunoprotein-chromatin complexes were captured by incubating with protein A-agarose beads (Santa Cruz Biotechnology), followed by consecutive washes in immunoprecipitation buffer and then elution as described (Gomez-Mena et al., 2005). Immunoprotein-DNA was then incubated consecutively in RNase A/T1 mix (Fermentas) and Proteinase K (Roche Diagnostics) as described, after which DNA was purified using Minelute columns (Qiagen) (Gomez-Mena et al., 2005). ChIP samples were tested for enrichment by qPCR and then deep sequencing libraries were produced by standard Illumina protocols.

ChIP-Seq Analysis

Standard Illumina base calling software was used to base call the 42 nucleotide sequence reads. We used SHORE (Ossowski et al., 2008) for read mapping and coverage analysis. The raw reads were pruned of low quality bases at their 3' end exactly as described (Ossowski et al., 2008) before mapping them to the unmasked TAIR9 genome using GenomeMapper (Schneeberger et al., 2009), allowing for up to four mismatching nucleotides and no gaps.

A two-step procedure was applied to the mapped reads to identify regions significantly enriched in the positive sample when compared with the control sample. First, a sliding window approach was used to identify potentially enriched candidate regions in the ChIP sample. Second, these genomic regions were quantified and used as an input to a statistical test to assess the significance of the enrichment in ChIP versus the control sample.

Briefly, using uniquely mapping reads only, we first calculated the fragment coverage graph for the genome (i.e., each position in the genome was annotated with the number of overlapping DNA fragments to obtain the coverage depth for each base). To achieve this, each read was extended in the 3' direction to 130 bp, corresponding to half the experimentally observed average fragment size of the immunoprecipitated DNA of ~200 to 300 bp. For detection of the described candidate peak regions, a 2-kb wide sliding window was applied to the fragment coverage graph. The sliding window was moved over the genome in single base steps, and in each step the potential enrichment of the central base was evaluated. Then, a one-sided Poisson test was applied, with the test parameter λ set to the local average coverage. This local average was calculated as the accumulated coverage values of all bases inside the 2-kb window, divided by the number of bases in the same range having a coverage value above zero. Positions with zero fragment

coverage were considered inaccessible by the ChIP experiment and thus were not included in the calculation. Any position whose coverage had a P value below 0.05 assigned by the Poisson test was considered a part of a potentially enriched region. For further analysis, we considered only consecutive stretches of positions with a P value below 0.05 that were longer than the approximate DNA fragment size of 130 bp. To reduce further the number of potentially enriched regions, we checked for unwarranted high average coverage in the control sample in each of these candidate regions. A candidate was discarded if the coverage mean in the control sample in the region corresponding to a potential peak in the positive sample was larger than the median average control coverage plus a tolerance of three standard deviations in the peak regions.

To assess the significance of the remaining enrichment candidates, a one-sided binomial test was applied to the read count data for each region. For any potential peak region, the test parameter N was set to the total number of reads mapping to the considered region in both the ChIP and the control assay. Using this test, a P value was assigned to the number of reads in the ChIP sample mapping to the region. To calculate the probability of success " r " required as a parameter for the binomial test, we first computed a scaling factor " s " for the control sample and the chromosome containing the considered region. The complete chromosome sequence was subdivided into 400-bp bins, and for each bin, the numbers of mapped reads for the positive sample as well as the control sample were recorded. Then, s was chosen such that the median ChIP sample read count for all bins equaled the median control sample read count multiplied by s . Using this, the binomial test parameter r was calculated as $r = s/(s + 1)$.

Finally, the resulting binomial test P values were transformed into FDRs using the Benjamini-Hochberg correction method. To provide further quality measures regarding the fidelity of peak regions, we also calculated the per base excess, which is defined as the excess of coverage averaged per base for the positive versus the control experiment ($[\text{chip reads} - (s * \text{control reads})] / \text{peak width}$). In the end, only peak regions with $\text{FDR} < 10^{-10}$ and a per base excess > 0.25 in both replicates were retained and are reported in Supplemental Data Set 1 online. We selected a particularly stringent FDR of 10^{-10} to limit our list of enriched regions to the most significant. This was employed as protection that our method might potentially underestimate the FDR for less significant regions. It is conceivable that using a binomial distribution to calculate P values could have the effect of producing low P values if it does not perfectly model the true tag distribution between experiment and control in every case, for example, if the variance of the true distribution is larger. Alternatively, it may be that AP2 binds an unusually large number of regions in the genome at a lower affinity. In any case, we chose to err on the side of higher peak calling stringency. ChIP-seq traces were visualized using GBrowse (Stein et al., 2002). All scripts and source code are available upon request.

EasyGO (Zhou and Su, 2007) was used to perform GO analysis.

Inducible AP2-GR Experiments

Since *ap2-2* plants do not grow well on selection media, *ap2-2* plants were genotyped for the transgene prior to chemical treatments. 35S: *AP2m3-GR ap2-2* seedlings were treated with 10 μ M CYC with or without 10 μ M DEX and 0.015% Silwet L-77 for 6 h. Four biological replicates were performed.

RNA Isolation and Blot Analysis

Dissected inflorescence tissue was obtained and total RNA isolation was performed using TRI reagent (Molecular Research Center). RNA gel blotting to detect microRNAs was done as previously described (Gy et al., 2007) with 6 μ g of total RNA. Hybridization was performed at 50°C in buffer containing $5 \times \text{SSC}$, 20 mM Na_2HPO_4 , pH 7.2, 7% SDS, and

2× Denhardt's solution. The 5'-end labeled (³²P) antisense oligonucleotides (see Supplemental Table 4 online) were used to detect miR156, miR172, and U6 (internal control). The membrane was washed with a solution containing 1× SSC and 1% SDS. Radioactive signals were then obtained and quantified using the Typhoon PhosphorImager system.

ChIP-Chip

Leaf tissue from 5-week-old plants was processed for ChIP as above, except we used an anti-GFP antibody (Abcam ab290). Raw ChIP was recovered and amplified using the Sigma-Aldrich WGA GenomePlex kit after we performed a comparison to other systems, which showed this protocol gives improved amplification consistency and minimal amplification bias, in accordance with a previous study (O'Geen et al., 2006). One microgram of DNA was fragmented, labeled, and hybridized to Affymetrix *Arabidopsis* tiling 1.0F arrays (Affymetrix). Chromatin size distribution and fragmentation performance was confirmed on an Agilent Bioanalyzer prior to array hybridization (Agilent Technologies).

Primary Tiling Array Analysis

Tiling array data were processed using the CisGenome suite (Ji et al., 2008). Briefly, raw .CEL files were quantile normalized, and peaks were called using TileMapv2. Analysis was performed in MA mode with window size 5, and only peaks detected with a FDR of better than 0.05 were analyzed. EasyGO was used to do gene ontology-based enrichment analysis (Zhou and Su, 2007). Genome-wide visualization was performed with Affymetrix Integrated Genome Browser after normalization with Affymetrix Tiling Array Software (Affymetrix).

Accession Numbers

Sequence data from this article can be found in the Arabidopsis Genome Initiative or GenBank/EMBL databases under the following accession numbers: AP2 (At4g36920), SMZ (At3g54990), SNZ (At2g39250), TOE1 (At2g28550), TOE2 (At5g60120), TOE3 (AT5G67180), AGL15 (AT5G13790), ARF3 (AT2G33860), CO (AT5G15840), FT (AT1G65480), TFL1 (AT5G03840), SOC1 (AT2G45660), FUL (AT5G60910), SEP3 (AT1G24260), AG (AT4G18960), SHP1 (AT3G58780), SHP2 (AT2G42830), STK (AT4G09960), AP1 (AT1G69120), miR156e (AT5G11977), and miR172b (AT5G04275). AP2 ChIP-seq data are available from the Gene Expression Omnibus database (GSE21301). AP2 tiling array data are freely available from the ArrayExpress database (E-MEXP-2653). AtGen-Express data on *Arabidopsis* development (Schmid et al., 2005) are available from The Arabidopsis Information Resource database.

Author Contributions

L.Y., M.S., J.M., F.O., T.D., and X.C. conceived of and designed the experiments. L.Y., T.D., J.M., M.S., and H.W. performed the experiments. L.Y., F.O., M.S., and T.D. analyzed the data. L.Y. and M.S. wrote the article.

Supplemental Data

The following materials are available in the online version of this article:

Supplemental Figure 1. AP2 mRNA Levels Are Decreased in *ap2-12*.

Supplemental Figure 2. Hexuple AP2-Like miR172 Target Mutant Exhibits Ectopic Activation of Flower Organ Identity Programs.

Supplemental Figure 3. Genome-Wide Physical Distribution of AP2-Bound Regions.

Supplemental Figure 4. Overlay of AG Amplicons Tested by qPCR with ChIP-Seq Data from Native AP2 Antibody ChIP-Seq.

Supplemental Figure 5. Gene Ontology of Target Sets Bound, Repressed, or Both Bound and Repressed by AP2.

Supplemental Figure 6. Induction of AP2-GR Promotes Late Flowering.

Supplemental Figure 7. AP2 mRNA Expression throughout *Arabidopsis thaliana* Development.

Supplemental Figure 8. ChIP-Chip Reveals AP2 Targets in Leaf Tissue during Functional Floral Repression.

Supplemental Figure 9. Comparison of AP2 Direct Targets in Different Tissues.

Supplemental Table 1. Flowering Time of *ap2*, miR172 Target Clade, and Photoperiod Pathway Mutants.

Supplemental Table 2. ChIP Sequencing and Mapping Summary.

Supplemental Table 3. Genomic Loci Containing Both AP2- and SMZ-Bound Regions.

Supplemental Table 4. Oligonucleotides Used in This Work.

Supplemental Table 5. Mutant Lines Used throughout This Work.

Supplemental Data Set 1. Excel Spreadsheet Containing Information on Chromosomal Regions That Were Significantly Enriched in the AP2 ChIP-Seq Experiment.

Supplemental Data Set 2. Excel Spreadsheet Containing Results from RankProducts Pairwise Comparisons (pfp < 0.01 or pfp < 0.1; 100 Permutations) between Genotypes.

Supplemental Data Set 3. AP2_Excel Spreadsheet Containing Information of the Overlap of Direct AP2 Targets Generated from Supplemental Data Sets 1 and 2.

Supplemental Data Set 4. Excel Spreadsheet Containing Information on Chromosomal Regions That Were Significantly Enriched in the AP2-GFP ChIP-Chip Experiment.

ACKNOWLEDGMENTS

We thank the Nottingham Arabidopsis Seed Centre for seeds. We also thank Schallum Werner for 35S:miR172 T1 seeds, Rebecca Schwab for the gift of a plasmid containing the AP2 open reading frame without stop codon, Patricia Springer for the pBI-GR-GW gateway destination vector, Jürgen Berger for assistance with scanning electron microscopy, members of the Schmid lab for discussion, and Detlef Weigel and Kirsten Bombliès-Yant for comments on the manuscript. F.O. was supported through BMBF-GABI Trilateral Grant TRANSNET to Detlef Weigel, H.W. was supported by a doctoral fellowship from Boehringer Ingelheim Fonds, and T.T.D. was supported by a National Science Foundation IGERT training grant (DGE0504249). This work was supported by a grant from the National Institutes of Health (GM61146) to X.C. and Deutsche Forschungsgemeinschaft grants (SCHM1560/3-1 and SCHM1560/5-1) to M.S. and the Max Planck Society.

Received March 31, 2010; revised July 7, 2010; accepted July 14, 2010; published July 30, 2010.

REFERENCES

Abe, M., Kobayashi, Y., Yamamoto, S., Daimon, Y., Yamaguchi, A., Ikeda, Y., Ichinoki, H., Notaguchi, M., Goto, K., and Araki, T. (2005). FD, a bZIP protein mediating signals from the floral pathway integrator FT at the shoot apex. *Science* **309**: 1052–1056.

- Adamczyk, B.J., Lehti-Shiu, M.D., and Fernandez, D.E. (2007). The MADS domain factors AGL15 and AGL18 act redundantly as repressors of the floral transition in Arabidopsis. *Plant J.* **50**: 1007–1019.
- Ahn, J.H., Miller, D., Winter, V.J., Banfield, M.J., Lee, J.H., Yoo, S.Y., Henz, S.R., Brady, R.L., and Weigel, D. (2006). A divergent external loop confers antagonistic activity on floral regulators FT and TFL1. *EMBO J.* **25**: 605–614.
- Alonso, J.M., et al. (2003). Genome-wide insertional mutagenesis of *Arabidopsis thaliana*. *Science* **301**: 653–657.
- Aukerman, M.J., and Sakai, H. (2003). Regulation of flowering time and floral organ identity by a MicroRNA and its APETALA2-like target genes. *Plant Cell* **15**: 2730–2741.
- Bombliès, K., Dagenais, N., and Weigel, D. (1999). Redundant enhancers mediate transcriptional repression of AGAMOUS by APETALA2. *Dev. Biol.* **216**: 260–264.
- Bowman, J.L., Smyth, D.R., and Meyerowitz, E.M. (1989). Genes directing flower development in *Arabidopsis*. *Plant Cell* **1**: 37–52.
- Bowman, J.L., Smyth, D.R., and Meyerowitz, E.M. (1991). Genetic interactions among floral homeotic genes of Arabidopsis. *Development* **112**: 1–20.
- Breitling, R., Armengaud, P., Amtmann, A., and Herzyk, P. (2004). Rank products: A simple, yet powerful, new method to detect differentially regulated genes in replicated microarray experiments. *FEBS Lett.* **573**: 83–92.
- Carrera, J., Rodrigo, G., Jaramillo, A., and Elena, S.F. (2009). Reverse-engineering the *Arabidopsis thaliana* transcriptional network under changing environmental conditions. *Genome Biol.* **10**: R96.
- Castillejo, C., and Pelaz, S. (2008). The balance between CONSTANS and TEMPRANILLO activities determines FT expression to trigger flowering. *Curr. Biol.* **18**: 1338–1343.
- Causier, B., Castillo, R., Zhou, J., Ingram, R., Xue, Y., Schwarz-Sommer, Z., and Davies, B. (2005). Evolution in action: Following function in duplicated floral homeotic genes. *Curr. Biol.* **15**: 1508–1512.
- Chae, K., Kieslich, C.A., Morikis, D., Kim, S.C., and Lord, E.M. (2009). A gain-of-function mutation of *Arabidopsis* lipid transfer protein 5 disturbs pollen tube tip growth and fertilization. *Plant Cell* **21**: 3902–3914.
- Chen, X. (2004). A microRNA as a translational repressor of APETALA2 in Arabidopsis flower development. *Science* **303**: 2022–2025.
- Corbesier, L., Vincent, C., Jang, S., Fornara, F., Fan, Q., Searle, I., Giakountis, A., Farrona, S., Gissot, L., Turnbull, C., and Coupland, G. (2007). FT protein movement contributes to long-distance signaling in floral induction of Arabidopsis. *Science* **316**: 1030–1033.
- Del Olmo, I., Lopez-Gonzalez, L., Martin-Trillo, M.M., Martinez-Zapater, J.M., Pineiro, M., and Jarillo, J.A. (2009). EARLY IN SHORT DAYS 7 (ESD7) encodes the catalytic subunit of DNA polymerase epsilon and is required for flowering repression through a mechanism involving epigenetic gene silencing. *Plant J.* **61**: 623–636.
- Deyholos, M.K., and Sieburth, L.E. (2000). Separable whorl-specific expression and negative regulation by enhancer elements within the AGAMOUS second intron. *Plant Cell* **12**: 1799–1810.
- Drews, G.N., Bowman, J.L., and Meyerowitz, E.M. (1991). Negative regulation of the Arabidopsis homeotic gene AGAMOUS by the APETALA2 product. *Cell* **65**: 991–1002.
- Fahlgren, N., Montgomery, T.A., Howell, M.D., Allen, E., Dvorak, S.K., Alexander, A.L., and Carrington, J.C. (2006). Regulation of AUXIN RESPONSE FACTOR3 by TAS3 ta-siRNA affects developmental timing and patterning in Arabidopsis. *Curr. Biol.* **16**: 939–944.
- Giakountis, A., and Coupland, G. (2008). Phloem transport of flowering signals. *Curr. Opin. Plant Biol.* **11**: 687–694.
- Gomez-Mena, C., de Folter, S., Costa, M.M., Angenent, G.C., and Sablowski, R. (2005). Transcriptional program controlled by the floral homeotic gene AGAMOUS during early organogenesis. *Development* **132**: 429–438.
- Gy, I., Gascioli, V., Laressergues, D., Morel, J.B., Gombert, J., Proux, F., Proux, C., Vaucheret, H., and Mallory, A.C. (2007). *Arabidopsis* FIERY1, XRN2, and XRN3 are endogenous RNA silencing suppressors. *Plant Cell* **19**: 3451–3461.
- Hanzawa, Y., Money, T., and Bradley, D. (2005). A single amino acid converts a repressor to an activator of flowering. *Proc. Natl. Acad. Sci. USA* **102**: 7748–7753.
- Heisler, M.G., Ohno, C., Das, P., Sieber, P., Reddy, G.V., Long, J.A., and Meyerowitz, E.M. (2005). Patterns of auxin transport and gene expression during primordium development revealed by live imaging of the Arabidopsis inflorescence meristem. *Curr. Biol.* **15**: 1899–1911.
- Hunter, C., Willmann, M.R., Wu, G., Yoshikawa, M., de la Luz Gutierrez-Nava, M., and Poethig, S.R. (2006). Trans-acting siRNA-mediated repression of ETTIN and ARF4 regulates heteroblasty in Arabidopsis. *Development* **133**: 2973–2981.
- Jaeger, K.E., Graf, A., and Wigge, P.A. (2006). The control of flowering in time and space. *J. Exp. Bot.* **57**: 3415–3418.
- Jaeger, K.E., and Wigge, P.A. (2007). FT protein acts as a long-range signal in Arabidopsis. *Curr. Biol.* **17**: 1050–1054.
- Ji, H., Jiang, H., Ma, W., Johnson, D.S., Myers, R.M., and Wong, W.H. (2008). An integrated software system for analyzing ChIP-chip and ChIP-seq data. *Nat. Biotechnol.* **26**: 1293–1300.
- Jung, J.H., Seo, Y.H., Seo, P.J., Reyes, J.L., Yun, J., Chua, N.H., and Park, C.M. (2007). The GIGANTEA-regulated microRNA172 mediates photoperiodic flowering independent of CONSTANS in Arabidopsis. *Plant Cell* **19**: 2736–2748.
- Kaufmann, K., Muino, J.M., Jauregui, R., Airoidi, C.A., Smaczniak, C., Krajewski, P., and Angenent, G.C. (2009). Target genes of the MADS transcription factor SEPALLATA3: Integration of developmental and hormonal pathways in the Arabidopsis flower. *PLoS Biol.* **7**: e1000090.
- Kaufmann, K., Wellmer, F., Muino, J.M., Ferrier, T., Wuest, S.E., Kumar, V., Serrano-Mislata, A., Madueño, F., Krajewski, P., Meyerowitz, E.M., Angenent, G.C., and Riechmann, J.L. (2010). Orchestration of floral initiation by APETALA1. *Science* **328**: 85–89.
- Kim, S., Soltis, P.S., Wall, K., and Soltis, D.E. (2006). Phylogeny and domain evolution in the APETALA2-like gene family. *Mol. Biol. Evol.* **23**: 107–120.
- Kobayashi, Y., and Weigel, D. (2007). Move on up, it's time for change—Mobile signals controlling photoperiod-dependent flowering. *Genes Dev.* **21**: 2371–2384.
- Komiya, R., Yokoi, S., and Shimamoto, K. (2009). A gene network for long-day flowering activates RFT1 encoding a mobile flowering signal in rice. *Development* **136**: 3443–3450.
- Kramer, E.M., Jaramillo, M.A., and Di Stilio, V.S. (2004). Patterns of gene duplication and functional evolution during the diversification of the AGAMOUS subfamily of MADS box genes in angiosperms. *Genetics* **166**: 1011–1023.
- Lee, J.H., Yoo, S.J., Park, S.H., Hwang, I., Lee, J.S., and Ahn, J.H. (2007). Role of SVP in the control of flowering time by ambient temperature in Arabidopsis. *Genes Dev.* **21**: 397–402.
- Li, D., Liu, C., Shen, L., Wu, Y., Chen, H., Robertson, M., Helliwell, C.A., Ito, T., Meyerowitz, E.M., and Yu, H. (2008). A repressor complex governs the integration of flowering signals in Arabidopsis. *Dev. Cell* **15**: 110–120.
- Lifschitz, E., Eviatar, T., Rozman, A., Shalit, A., Goldshmidt, A., Amsellem, Z., Alvarez, J.P., and Eshed, Y. (2006). The tomato FT ortholog triggers systemic signals that regulate growth and flowering and substitute for diverse environmental stimuli. *Proc. Natl. Acad. Sci. USA* **103**: 6398–6403.
- Liljegren, S.J., Ditta, G.S., Eshed, Y., Savidge, B., Bowman, J.L., and Yanofsky, M.F. (2000). SHATTERPROOF MADS-box genes control seed dispersal in Arabidopsis. *Nature* **404**: 766–770.

- Liu, C., Xi, W., Shen, L., Tan, C., and Yu, H. (2009). Regulation of floral patterning by flowering time genes. *Dev. Cell* **16**: 711–722.
- Liu, F., Marquardt, S., Lister, C., Swiezewski, S., and Dean, C. (2010). Targeted 3' processing of antisense transcripts triggers Arabidopsis FLC chromatin silencing. *Science* **327**: 94–97.
- Mathieu, J., Warthmann, N., Kuttner, F., and Schmid, M. (2007). Export of FT protein from phloem companion cells is sufficient for floral induction in Arabidopsis. *Curr. Biol.* **17**: 1055–1060.
- Mathieu, J., Yant, L.J., Murdter, F., Kuttner, F., and Schmid, M. (2009). Repression of flowering by the miR172 target SMZ. *PLoS Biol.* **7**: e1000148.
- Melzer, S., Lens, F., Gennen, J., Vanneste, S., Rohde, A., and Beeckman, T. (2008). Flowering-time genes modulate meristem determinacy and growth form in *Arabidopsis thaliana*. *Nat. Genet.* **40**: 1489–1492.
- O'Geen, H., Nicolet, C.M., Blahnik, K., Green, R., and Farnham, P.J. (2006). Comparison of sample preparation methods for ChIP-chip assays. *Biotechniques* **41**: 577–580.
- Ohto, M., Onai, K., Furukawa, Y., Aoki, E., Araki, T., and Nakamura, K. (2001). Effects of sugar on vegetative development and floral transition in Arabidopsis. *Plant Physiol.* **127**: 252–261.
- Ohto, M.A., Fischer, R.L., Goldberg, R.B., Nakamura, K., and Harada, J.J. (2005). Control of seed mass by APETALA2. *Proc. Natl. Acad. Sci. USA* **102**: 3123–3128.
- Okamoto, J.K., Caster, B., Villarreal, R., Van Montagu, M., and Jofuku, K.D. (1997). The AP2 domain of APETALA2 defines a large new family of DNA binding proteins in Arabidopsis. *Proc. Natl. Acad. Sci. USA* **94**: 7076–7081.
- Ossowski, S., Schneeberger, K., Clark, R.M., Lanz, C., Warthmann, N., and Weigel, D. (2008). Sequencing of natural strains of *Arabidopsis thaliana* with short reads. *Genome Res.* **18**: 2024–2033.
- Park, W., Li, J., Song, R., Messing, J., and Chen, X. (2002). CARPEL FACTORY, a Dicer homolog, and HEN1, a novel protein, act in micro-RNA metabolism in *Arabidopsis thaliana*. *Curr. Biol.* **12**: 1484–1495.
- Pinyopich, A., Ditta, G.S., Savidge, B., Liljegren, S.J., Baumann, E., Wisman, E., and Yanofsky, M.F. (2003). Assessing the redundancy of MADS-box genes during carpel and ovule development. *Nature* **424**: 85–88.
- Pouteau, S., Ferret, V., Gaudin, V., Lefebvre, D., Sabar, M., Zhao, G., and Prunus, F. (2004). Extensive phenotypic variation in early flowering mutants of Arabidopsis. *Plant Physiol.* **135**: 201–211.
- Schmid, M., Davison, T.S., Henz, S.R., Pape, U.J., Demar, M., Vingron, M., Scholkopf, B., Weigel, D., and Lohmann, J.U. (2005). A gene expression map of *Arabidopsis thaliana* development. *Nat. Genet.* **37**: 501–506.
- Schmid, M., Uhlenhaut, N.H., Godard, F., Demar, M., Bressan, R., Weigel, D., and Lohmann, J.U. (2003). Dissection of floral induction pathways using global expression analysis. *Development* **130**: 6001–6012.
- Schneeberger, K., Hagmann, J., Ossowski, S., Warthmann, N., Gesing, S., Kohlbacher, O., and Weigel, D. (2009). Simultaneous alignment of short reads against multiple genomes. *Genome Biol.* **10**: R98.
- Schwab, R., Palatnik, J.F., Riester, M., Schommer, C., Schmid, M., and Weigel, D. (2005). Specific effects of microRNAs on the plant transcriptome. *Dev. Cell* **8**: 517–527.
- Sessions, A., Nemhauser, J.L., McColl, A., Roe, J.L., Feldmann, K.A., and Zambryski, P.C. (1997). ETTIN patterns the Arabidopsis floral meristem and reproductive organs. *Development* **124**: 4481–4491.
- Simpson, G.G., Quesada, V., Henderson, I.R., Dijkwel, P.P., Macknight, R., and Dean, C. (2004). RNA processing and Arabidopsis flowering time control. *Biochem. Soc. Trans.* **32**: 565–566.
- Sohn, E.J., Rojas-Pierce, M., Pan, S., Carter, C., Serrano-Mislata, A., Madueno, F., Rojo, E., Surpin, M., and Raikhel, N.V. (2007). The shoot meristem identity gene TFL1 is involved in flower development and trafficking to the protein storage vacuole. *Proc. Natl. Acad. Sci. USA* **104**: 18801–18806.
- Stein, L.D., Mungall, C., Shu, S., Caudy, M., Mangone, M., Day, A., Nickerson, E., Stajich, J.E., Harris, T.W., Arva, A., and Lewis, S. (2002). The generic genome browser: A building block for a model organism system database. *Genome Res.* **12**: 1599–1610.
- Swiezewski, S., Liu, F., Magusin, A., and Dean, C. (2009). Cold-induced silencing by long antisense transcripts of an Arabidopsis Polycomb target. *Nature* **462**: 799–802.
- Tamaki, S., Matsuo, S., Wong, H.L., Yokoi, S., and Shimamoto, K. (2007). Hd3a protein is a mobile flowering signal in rice. *Science* **316**: 1033–1036.
- Wang, J.W., Czech, B., and Weigel, D. (2009). miR156-regulated SPL transcription factors define an endogenous flowering pathway in *Arabidopsis thaliana*. *Cell* **138**: 738–749.
- Wigge, P.A., Kim, M.C., Jaeger, K.E., Busch, W., Schmid, M., Lohmann, J.U., and Weigel, D. (2005). Integration of spatial and temporal information during floral induction in Arabidopsis. *Science* **309**: 1056–1059.
- Willis, C.G., Ruhfel, B., Primack, R.B., Miller-Rushing, A.J., and Davis, C.C. (2008). Phylogenetic patterns of species loss in Thoreau's woods are driven by climate change. *Proc. Natl. Acad. Sci. USA* **105**: 17029–17033.
- Wu, G., Park, M.Y., Conway, S.R., Wang, J.W., Weigel, D., and Poethig, R.S. (2009). The sequential action of miR156 and miR172 regulates developmental timing in Arabidopsis. *Cell* **138**: 750–759.
- Wu, Z., Irizarry, R.A., Gentleman, R., Martinez-Murillo, F., and Spencer, F. (2004). A model-based background adjustment for oligonucleotide expression arrays. *J. Am. Stat. Assoc.* **99**: 909–917.
- Wurschum, T., Gross-Hardt, R., and Laux, T. (2006). APETALA2 regulates the stem cell niche in the *Arabidopsis* shoot meristem. *Plant Cell* **18**: 295–307.
- Yant, L., Mathieu, J., and Schmid, M. (2009). Just say no: Floral repressors help Arabidopsis bide the time. *Curr. Opin. Plant Biol.* **12**: 580–586.
- Zhao, L., Kim, Y., Dinh, T.T., and Chen, X. (2007). miR172 regulates stem cell fate and defines the inner boundary of APETALA3 and PISTILLATA expression domain in *Arabidopsis* floral meristems. *Plant J.* **51**: 840–849.
- Zheng, Y., Ren, N., Wang, H., Stromberg, A.J., and Perry, S.E. (2009). Global identification of targets of the *Arabidopsis* MADS domain protein AGAMOUS-Like15. *Plant Cell* **21**: 2563–2577.
- Zhou, X., and Su, Z. (2007). EasyGO: Gene Ontology-based annotation and functional enrichment analysis tool for agronomical species. *BMC Genomics* **8**: 246.